JOURNAL OF MECHANICAL ENGINEERING AND SCIENCES
ISSN: 2289-4659 e-ISSN: 2231-8380
VOLUME 19, ISSUE 1, 2025, 10521 - 10529
DOI: https://doi.org/10.15282/jmes.19.1.2025.7.0824

RESEARCH ARTICLE

Deep learning segmentation of brain ischemic lesion from magnetic resonance images for three-dimensional modelling

M. I. Mat Lizah[1], N. H. Johari[2], M. J. Mohamed Mokhtarudin[1]*

[1] Faculty of Manufacturing and Mechatronic Engineering Technology, Universiti Malaysia Pahang Al-Sultan Abdullah, 26600 Pekan, Pahang, Malaysia
Phone: +6094316179
[2] Faculty of Mechanical and Automotive Engineering Technology, Universiti Malaysia Pahang Al-Sultan Abdullah, 26600 Pekan, Pahang, Malaysia

ABSTRACT - Automated segmentation is important for early detection and treatments to reduce disability and death risks among brain stroke patients. The existing segmentation algorithm is limited due to its computationally expensiveness in achieving a small accuracy. This work aims to develop a computationally economical automated brain infarct segmentation from T1-weighted Magnetic Resonance Imaging (MRI) using convolutional neural network architecture U-Net, but with reasonable accuracy compared to existing algorithm. The data used is taken from the Anatomical Tracing of Lesion After Stroke (ATLAS) open-source dataset, consisting of 304 brain t1-weigthed MRI images. The data is divided into training, test, and validation sets according to the 8:1:1 ratio. The data is then pre-processed so that all of them have similar size for the U-Net input. Then, the U-Net architecture is generated using encoder depth of 7. Certain hyperparameters including the number of epochs, encoder depth, and optimizers are varied. The U-Net with encoder depth 7 and using Adam optimizer gives the highest accuracy and loss, which are 92.33% and 0.9771, respectively. Further comparison with previous works shows that the present U-Net beaten the regular U-Net and also gives relatively similar accuracy and loss. Future improvements on the present U-Net is necessary so that the accuracy can be increased further, computationally economic, and to produce a near accurate semantic segmentation of brain lesion.

ARTICLE HISTORY
Received : 13th Aug. 2024
Revised : 28th Dec. 2024
Accepted : 08th Mar. 2025
Published : 30th Mar. 2025

KEYWORDS
Brain stroke
Image segmentation
Deep learning
Brain modelling

1. INTRODUCTION

In recent years, deep neural networks have outperformed other machine learning techniques in visual recognition tasks [1]. The success of neural networks has been limited due to the lack of datasets, which prevents the use of a complex network [2]. The method developed by Krizhevsky et al. [1] proposed a large network on ImageNet dataset with millions of training images, which created more idea for even larger and deeper neural networks [3]. In medical image processing, the desired output upon a segmentation process should include the identification and localization of a certain abnormality, in which each pixel is assigned with a class label of either normal or abnormal. In addition, biomedical images are usually limited. Therefore, the works by [4, 5] utilized a sliding-window setup to perform the prediction and produce a localize patch. This patch can produce a larger number of training images from the available biomedical images. A more recent advancement of image identification technique utilizing a large network known as convolutional neural network (CNN) has shown a remarkable potential in medical image segmentation task [6]. A specialized CNN architecture known as the U-Net has been developed to perform medical image segmentation to separate the abnormality including tumor, brain infarct, and many others [7].

Semantic segmentation is the ability for a computer to classify a feature in each image pixel-by-pixel. In this project, the brain stroke lesion MRI images from the Anatomical Tracings of Lesions After Stroke (ATLAS) will be used. Brain stroke is usually diagnosed using medical imaging modalities such as computed tomography (CT) and magnetic resonance imaging (MRI). The lesion formed after a stroke attack indicates the location of malfunction brain tissue. Different clinicians and research groups use various modalities to obtain their data and this creates problem in reproducing their findings using the different techniques they have developed [8]. In addition, these groups also have datasets with variety of image orientations and qualities, which make the image analysis to be specific for particular research groups. Therefore, there is a need to develop a common brain stroke image analysis utilizing various datasets among different groups.

Manual segmentation of brain stroke lesion by radiologist has been used as the gold standard despite of its accuracy is only about 73% [9]. Therefore, automatic segmentation of brain stroke lesion is essential to reduce the workload for manual segmentation and improve the accuracy. ATLAS is a collection of datasets from various research groups with common image orientation and qualities and this dataset is made available for researchers to develop their own segmentation technique [10]. Medical image segmentation is important, especially for evaluating a particular disease using patient-specific finite element modelling [11]. However, manual segmentation is tedious and a slow process.

*CORRESPONDING AUTHOR | M. J. Mohamed Mokhtarudin | ✉ mohdjamil@umpsa.edu.my

Therefore, this paper aims to develop an automatic image segmentation algorithm on brain stroke lesion MRI using CNN, specifically the U-Net architecture. Furthermore, the algorithm should be able to be trained using economical computational resources. The success of this image segmentation will enable the processing of the images into three-dimensional (3D) model, which later could be used in finite element simulation.

2. MATERIALS AND METHODS

2.1 Brain Stroke Lesion Data

The data use in this study is taken from the ATLAS open-source dataset [10], which consists of 304 T1-weighted MRI scans of brain stroke patients. Generally, the data were taken from 11 cohorts of chronic-stroke patients worldwide. The data also contains manual segmentation of the lesion that was done by expert radiologists. 58% of the data contains at least one lesion, while the remaining data have multiple lesions [9].

2.2 Image Pre-processing

Before the U-Net can be trained, the ATLAS data must be pre-processed. The data has different sizes and pixel values [12]. Therefore, pre-processing is needed and is done in two steps, which are: (1) data resizing and (2) data scaling. Firstly, all of the images are resized into 256×256×128 from their original sizes. Then, the images undergo scaling process by converting the images into grayscale, in which each pixel value is converted to have a value within the range of 0 and 1.

2.3 U-Net Architecture

U-Net is an example of CNN that was created for image segmentation work [5, 13, 14]. The U-Net used in this study is mostly unchanged from the original model developed in [5], which has similar architecture as in Figure 1 [15]. The down-sampling path of the network consists of a convolution, a rectified linear unit (ReLU) function, and a max pooling operation, which doubles the number of features at each down-sampling step. This is then followed by up-sampling process with similar processes but reverse from the down-sampling steps. The final layer uses a 1x1 convolution operation to map the feature to the number of classes, which is one for this study.

The U-Net consists of 8 encoder depth, which can be calculated using Eq. (1):

$$\text{Image Size} = 2^{\text{Encoder Depth}} \tag{1}$$

The input image size is 256×256×128, hence the encoder depth is 8 following the image size 256. The pixel labels can be predicted by forward propagation without mirroring the input image and to avoid overfitting, as has been done in [5].

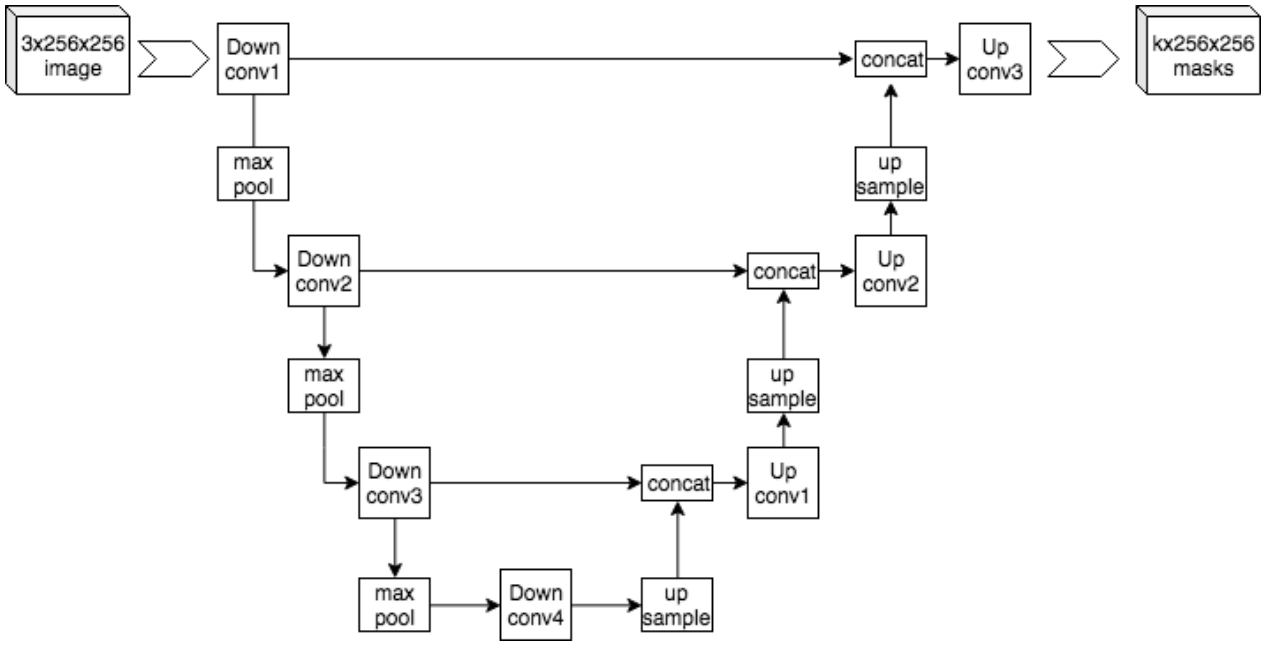

Figure 1. An example of U-Net architecture [15]

2.4 Parameter Initialization Optimizer

The training algorithm is iterative for the U-Net model. In this study, the Stochastic Gradient Descent with Momentum (SGDM) and Adaptive Moment Estimation (Adam) were used, in determining the new weights, θ_{l+1} from the previous weights, θ_l. Both SGDM and Adam were used and then comparison was performed to determine the best optimizer. Each of the optimizer is described in the following subsections.

2.4.1 Stochastic Gradient Descent with Momentum (SDGM)

The SGDM update is given by Eq. (2):

$$\theta_{l+1} = \theta_l - \alpha \nabla E(\theta_l) + \gamma(\theta_l - \theta_{l-1}) \tag{2}$$

where, γ determines the contribution of the previous gradient step to the current iteration.

2.4.2 Adam

The Adam update is given by Eqs. (3) and (4):

$$m_l = \beta_1 m_{l-1} + (1 - \beta_1)\nabla E(\theta_l) \tag{3}$$

$$v_l = \beta_2 v_{l-1} + (1 - \beta_1)[\nabla E(\theta_l)]^2 \tag{4}$$

where β_1 and β_2 are decay rates. Adam uses the moving averages to update the network parameters as in Eq. (5):

$$\theta_{l+1} = \theta_l - \frac{\alpha m_l}{\sqrt{v_l} + \epsilon} \tag{5}$$

2.5 Loss Function

Brain stroke lesion pixel within the whole brain image covers only a small fraction. Therefore, segmenting the lesion from the background is a highly computational task. The dice loss function is used here to determine the accuracy during the training procedure. The generalized dice loss function, L, used in the U-Net for calculating the loss between one image, Y and the corresponding ground truth, T is given by Eq. (6):

$$L = 1 - \frac{2\sum_{k=1}^{K} w_k \sum_{m=1}^{M} Y_{km} T_{km}}{\sum_{k=1}^{K} w_k \sum_{m=1}^{M} Y_{km}^2 + T_{km}^2} \tag{6}$$

where, K is the number of classes, M is the number of elements along the first two dimension of Y, and w_k is a class specific weighting factor that control the contribution each class makes to the loss.

2.6 Object-level Loss

Loss function acts on the pixel level, but this does not correlate with the segmentation performance. Thus, the dice coefficient is calculated to account for this is given by Eq. (7):

$$\text{Dice coefficient}(A, B) = 2\frac{|A \cap B|}{|A| + |B|} \tag{7}$$

here, A and B represent the ground truth area and the prediction area, respectively. The intersection of A and B is the true positive.

2.7 Training Procedure

Each epoch will be trained for 60 iterations for a total of 10 epochs. Each iteration will be trained using a minibatch size of 4. The initial learning rate used is 0.01. The data were divided into 3 sets with a ratio of 8:1:1 into training, testing, and validation sets. Overall, the data is divided into 243 for training, 31 for testing, and 31 for validation.

2.8 Computer Specifications

The computer specifications is as shown in Table 1, where the U-Net is trained using a Graphic Processing Unit (GPU) [16]. The GPU used is an economical GPU, which has a total of 6GB VRAM, and constructed with 3.8 GHz CPU with 4 cores.

Table 1. Computer specification

Component	Specification
Central Processing Unit (CPU)	AMD Ryzen 3 3300x (3.8Ghz clock speed), 4 cores
Random-Access Memory (RAM)	16GB DDR4 – 2400MHz
Graphic Processing Unit (GPU)	RTX 2060
Video Random-Access Memory (VRAM)	6GB VRAM

2.9 Evaluation Metric

Pixel accuracy and intersection over union (IoU) are the metrics used for measuring the accuracy of the image segmentation. IoU is the intersection of pixels predicted and the ground truth pixels divided by the union of the pixels predicted and ground truth pixels. The average IoU is given by Eq. (8):

$$M_{iou} = \left(\frac{1}{N_c}\right)\frac{\sum_i n_{ii}}{t_i + \sum_j n_{ji} - n_{ii}} \tag{8}$$

where, n_{ij} represents the number of pixels of class i predicted to be class j, N_c is the number of classes and $t_i = \sum_j n_{ij}$. Figure 2 shows an illustration to determine the IoU.

Meanwhile, pixel accuracy is the total number of pixels that is correctly predicted over the total number of pixels in an image, which is given by Eq. (9):

$$\text{Pixel}_{\text{accuracy}} = \frac{\sum_i n_{ii}}{\sum_i t_i} \tag{9}$$

To calculate evaluation metric, the test image and trained U-Net are used to identify the location of stroke lesion in MRI test image. Then, the calculation of the evaluation metrics will be conducted between the predicted label and ground truth label images.

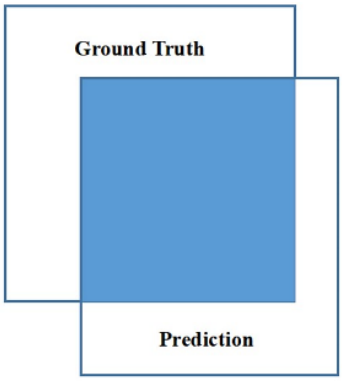

Figure 2. Examples of intersections over union

3. RESULTS AND DISCUSSION

3.1 Image Data

Figure 3 shows an example of pre-processed image, which has been resized into 256×256 resolutions and gray scaled. The voxels are represented by 8-bit integers.

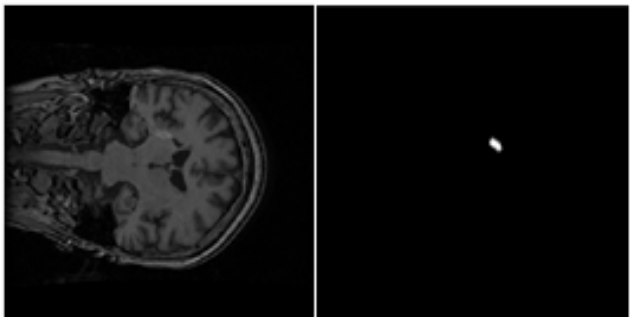

(a) (b)

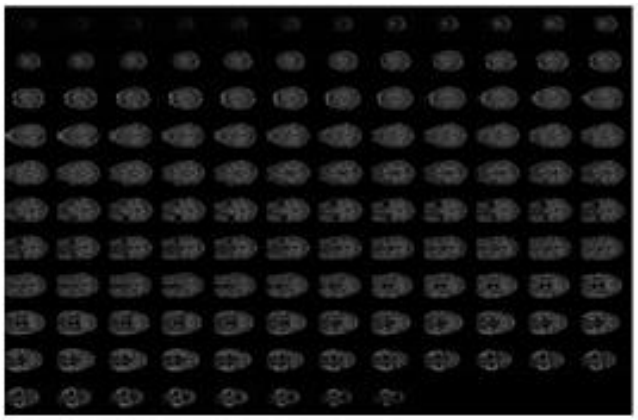

(c)

Figure 3. (a) Image for brain, (b) lesion and (c) after pre-processing and 128 slices of the image

3.2 Training Results

The U-Net 1 was trained using the hyperparameters as shown in Table 2. The first run is to find whether the U-Net accuracy has achieved constant learning based on the accuracy graph. The U-Net takes 163 minutes to complete the training. The accuracy achieve is 62.59% and loss at 0.9963. There is still a little increase in accuracy after epoch 7 to 10. The epoch was increase the to 30 while using the same hyperparameters. By increasing epoch of the U-Net learning, it can be seen the U-Net accuracy becomes constant as the epoch increases. Then, the hyperparameters were changed according to Table 2 for U-Net 2. The training time for is around 539 minutes. Final accuracy achieve is 62.71% and loss is 0.9924. By increasing the epoch up to 30, there is a little increase in accuracy. However, the training achieves its constant accuracy and loss before it reaches epoch 10. Thus, using only 10 epochs is enough and can reduce the training time.

Table 2. Hyperparameters used for U-Net 3

Name	U-Net 1	U-Net 2	U-Net 3	U-Net 4	U-Net 5
Input Size	256 × 256 ×128 × 1	256 x 256 x 128 x 1	256 x 256 x 128 x 1	256 x 256 x 128 x 1	256 x 256 x 128 x 1
Mini Batch Size	4	4	4	4	4
Learning Rate	0.01	0.01	0.01	0.01	0.01
Optimizer	SGDM	SGDM	SGDM	SGDM	Adam
Epoch	10	30	10	10	10
Encoder Depth	6	5	6	7	7

Next, the U-Net 3 was trained by changing the encoder depth of the U-Net with the same hyperparameters as U-Net 1, as shown in Table 2. Increasing the depth corresponds to adding an additional convolutional layer to the encoder as well as to the decoder. Increasing the depth layer by 1 has increase the learning accuracy and lowering the loss during training. The final accuracy and loss of U-Net 3 is 67.78% and 0.981, respectively. The training duration is 166 minutes. Then, the depth was further increase to 7, as shown in Table 2. U-Net 4 achieved 82.90% accuracy and 0.977 loss, while the training time is 167 minutes, and this is the maximum encoder depth that can be used. Further, the different optimizers were compared, by changing it to Adam. Table 2 shows the hyperparameters for U-Net 5 using Adam and with depth 7. Using Adam increases the accuracy up to 92.33% and loss at 0.9771 with 161 minutes of training time. It should be noted that the maximum depth that can be used is 7 due to the constraints by the hardware in terms of VRAM and processor. The learning rate remained unchanged. However, the learning rate drop factor was used. Learning rates drop factor is a multiplicative factor to apply to the learning rate every time a certain number of epochs passes. In our case, our training network initial learning rate start at 0.01 and end at 0.001. Table 3 summarises the accuracy and loss of the different optimizer and depth used in our U-Net.

Table 3. Accuracy and loss for different U-Net depth and optimizer

Optimizer	Depth	Accuracy	Loss
SGDM	5	62.59%	0.9963
SGDM	6	67.78%	0.9810
SGDM	7	82.90%	0.9770
Adam	7	92.33%	0.9771

3.3 Image Semantic Segmentation Result

The image segmentation for both optimizer Adam and SDGM are compared. Both optimizers have high accuracy with depth 7 as shown in Table 4. Figures 4 and 5 show an example of image after the segmentation process using the U-Net developed here. The left images are the ground truth, while the right images are the predicted segmentations using the U-Net. Table 4 shows the evaluation of the two U-Net used with different optimizers. From this table, it can be observed that U-Net with Adam outperformed U-Net with SDGM in all metrics. However, both U-Net have lower dice score.

Table 4. Metrics comparison between U-Net with SDGM and U-Net with Adam

Evaluation	U-Net with SDGM	U-Net with Adam
Pixel accuracy	0.9961	0.9996
Mean accuracy	0.6635	0.7946
Mean IoU	0.6152	0.7088
Dice similarity	0.3797	0.5895

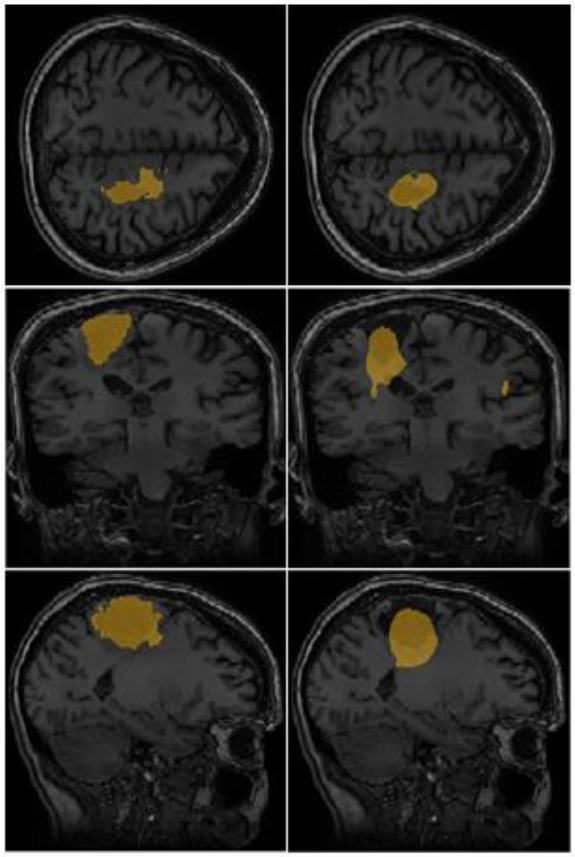

Figure 4. Segmentation result of one example test image using U-Net with SGDM optimizer. The left side is ground truth and right side is network prediction

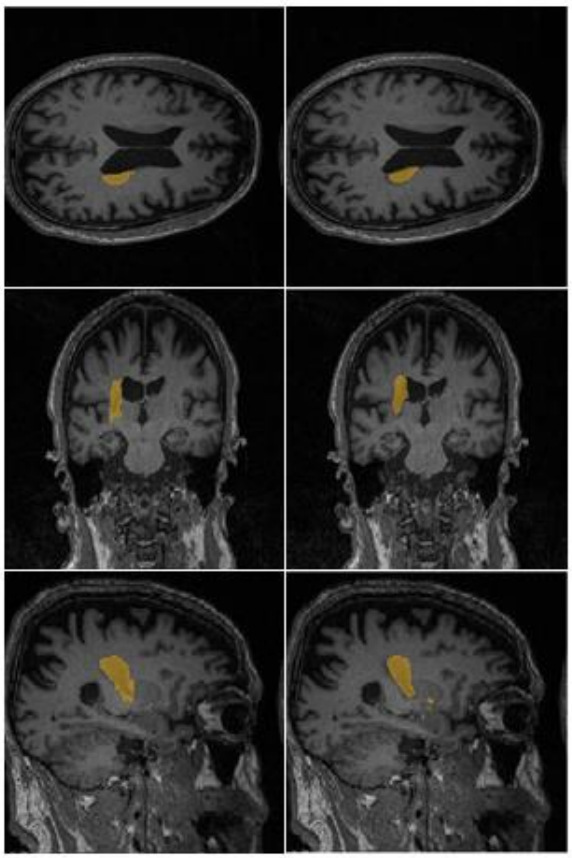

Figure 5. Segmentation result of one example test image using U-Net with Adam optimizer. The left side is ground truth and right side is network prediction

3.4 Comparison between the Proposed U-Net and Other Model

Table 5 shows the comparison of the proposed U-Net with other models found in the literature, such as the original U-Net [5], Improved U-Net [17], DeepLab v3+ [18], and MSDF [19]. It can be observed that proposed model has higher dice similarity than the original U-Net model, but lower compared to another neural network models, which has been modified to efficiently segment the brain MRI. The experimental results in stroke lesion segmentation show that all results have close result in term of dice efficiency. A dice similarity near 1.00 is desirable. However, all existing models, including the proposed U-Net, have dice similarity below 0.7, and this requires further model improvement to achieve better results. Despite this, our U-Net can be trained using economical processors with reasonable training time.

Table 5. Comparison of dice similarity between the Proposed U-Net and other models

Model	Dice Similarity
Original U-Net	0.4791
Our U-Net	0.5896
Improved U-Net	0.5930
DeepLab v3+	0.6220
MSDF-Net	0.6875

3.5 Limitations and Future Improvements

An automatic segmentation of brain stroke lesion images has been developed utilizing CNN method using U-Net architecture. The proposed U-Net managed to obtain accuracy of 58.96%, which is more than the U-Net developed from previous works [5]. Even though this accuracy is less than other segmentation models, the proposed U-Net can be trained using an economical computing setup. However, further improvements can be made to ensure better segmentation accuracy. The other segmentation algorithms that were compared with our U-Net, which are the improved U-Net, DeepLab v3+, and MSDF, were developed by adding additional features to the original U-Net. These additional features allow for improved segmentation [18, 19]. However, adding extra features only increases the accuracy by an additional 10% from our U-Net. There are other variations of U-Net for medical image segmentation with different purposes. For example, the modified U-Net developed in [20, 21] performed image segmentation by convoluting the images in 2D and 3D separately, and then combines the information obtained. This enables the process to use less computational resources. Furthermore, the work by [22] developed a version of U-Net that can perform segmentation to differentiate the brain tissue with image background and noise that have similar grayscale characteristics. Although the examples given may not improve the segmentation accuracy, they could help to improve the segmentation performance and utilization of computational resources.

The amount of brain images presented by the open-source data ATLAS is only 304, which all comprise of MRI images. However, most of the time, CT scans were used as the first medical imaging for diagnosing brain stroke. The image quality of CT and MRI is different [23]. A segmentation algorithm should be able to perform well for images obtained via cross-domain [24]. Therefore, additional data is needed to ensure that the segmentation algorithm could perform well. To ensure standardization of brain stroke imaging data, The Stroke Imaging Research (STIR) group has collected sets of brain stroke imaging data from various clinical trials [25]. The segmented brain images could then be developed into 3D geometry and be used in finite element simulations with suitable mathematical models [26-28]. Other than segmenting the brain and the stroke lesion, the brain lateral ventricles are also needed, especially in evaluating the brain herniation [26, 28, 29]. Methodology for ventricular segmentation have been well established and various algorithms have been developed [30]. Combining both brain stroke lesion and ventricular segmentation could enhance the efficacy of brain image segmentation and modelling.

4. CONCLUSIONS

A new U-Net model has been proposed to perform 3D brain image stroke lesion segmentation. Furthermore, several hyperparameters including optimizers, encoder depth, and epoch were manipulated to determine the best U-Net setup. From this study, it was found that the U-Net with encoder depth 7 and utilizing Adam optimizer performs the best lesion segmentation. Further comparison of the proposed model with existing U-Net and modified models has shown the potential of the proposed model in matching the performance of previous models. There are several improvements that can be made to further this research. One of the improvements is to develop a more effective loss function that can differentiate the background from the lesion. Another improvement is to develop a modified U-Net architecture but utilizing the Adam optimizer, which has been proven better compared to the SDGM.

ACKNOWLEDGEMENTS

This research is supported by the Universiti Malaysia Pahang Al-Sultan Abdullah International Publication grant (Grant ID: RDU203302)

CONFLICT OF INTEREST

The authors declare no conflicts of interest.

AUTHORS CONTRIBUTION

M. I. Mat Lizah (Methodology; Formal analysis; Visualisation; Writing – original draft)

N. H. Johari (Writing – proofread; Supervision)

M. J. Mohamed Mokhtarudin (Conceptualization; Writing – proof read; Supervision)

AVAILABILITY OF DATA AND MATERIALS

The data supporting this study's findings are available on request from the corresponding author.

ETHICS STATEMENT

Not applicable.

REFERENCES

[1] A. Krizhevsky, I. Sutskever, G. E. Hinton, "ImageNet classification with deep convolutional neural networks," *Communications of the ACM*, vol. 60, no. 6, pp. 84–90, 2017.

[2] Y. LeCun, B. Boser, J. S. Denker, D. Henderson, R. E. Howard, W. Hubbard, L. D. Jackel, "Backpropagation applied to handwritten zip code recognition," *Neural Computation*, vol. 1, no. 4, pp. 541-551, 1989.

[3] K. Simonyan, "Large-scale learning of discriminative image representations," *Ph.D. Thesis*, University of Oxford, United Kingdom, 2013.

[4] D. C. Cireşan, A. Giusti, L. M. Gambardella, & J. Schmidhuber, "Mitosis detection in breast cancer histology images with deep neural networks," in *Medical Image Computing and Computer-Assisted Intervention (MICCAI 2013)*, pp. 411-418, 2013.

[5] O. Ronneberger, P. Fischer, T. Brox, "U-Net: Convolutional networks for biomedical image segmentation," in *Medical Image Computing and Computer-Assisted Intervention (MICCAI 2015)*, pp. 234-241, 2015.

[6] K. Qi, H. Yang, C. Li, Z. Liu, M. Wang, Q. Liu, et al., "X-Net: Brain stroke lesion segmentation based on depthwise separable convolution and long-range dependencies," in *Medical Image Computing and Computer Assisted Intervention (MICCAI 2019)*, pp 247-255, 2019.

[7] B. Zhang, Y. Wang, C. Ding, Z. Deng, L. Li, Z. Qin, et al., "Multi-scale feature pyramid fusion network for medical image segmentation," *International Journal of Computer Assisted Radiology and Surgery*, vol. 18, no. 2, pp. 353-365, 2023.

[8] K. L. Ito, A. Kumar, A. Zavaliangos-Petropulu, S. C. Cramer, S. -L. Liew, "Pipeline for analyzing lesions after stroke (PALS)," *Frontiers in Neuroinformatics*, vol. 12, pp. 1-12, 2018.

[9] Y. Zhang, J. Wu, Y. Liu, Y. Chen, E. X. Wu, X. Tang, "MI-UNet: Multi-inputs UNet incorporating brain parcellation for stroke lesion segmentation from T1-weighted magnetic resonance images," *IEEE Journal of Biomedical and Health Informatics*, vol. 25, no. 2, pp. 526-535, 2021.

[10] S. -L. Liew, J. M. Anglin, N. W. Banks, M. Sondag, K. L. Ito, H. Kim, et al., "A large, open source dataset of stroke anatomical brain images and manual lesion segmentations," *Scientific Data*, vol. 5, p. 180011, 2018.

[11] M. J. Mohamed Mokhtarudin, A. Shabudin, S. J. Payne, "Effects of brain tissue mechanical and fluid transport properties during ischaemic brain oedema: A poroelastic finite element analysis," in *IEEE-EMBS Conference on Biomedical Engineering and Sciences (IECBES)*, pp. 1-6, 2018.

[12] K. Kipli, A. Z. Kouzani, "Degree of contribution (DoC) feature selection algorithm for structural brain MRI volumetric features in depression detection," *International Journal of Computer Assisted Radiology and Surgery*, vol. 10, no. 7, pp. 1003-1016, 2015.

[13] T. Shelatkar, D. Urvashi, M. Shorfuzzaman, A. Alsufyani, K. Lakshmanna, "Diagnosis of brain tumor using light weight deep learning model with fine-tuning approach," *Computational and Mathematical Methods in Medicine*, vol. 2022, no. 1, pp. 1-9, 2022.

[14] W. Sun, R. Wang, "Fully convolutional networks for semantic segmentation of very high resolution remotely sensed images combined with DSM," *IEEE Geoscience and Remote Sensing Letters*, vol. 15, no. 3, pp. 474-478, 2018.

[15] M. Yazdani, "An Example of Architecture of U-Net," Wikimedia Commons [Online], 2019. Available: https://commons.wikimedia.org/w/index.php?curid=81055729

[16] S. Choi, K. Lee, "A CUDA-based implementation of convolutional neural network," in *4th International Conference on Computer Applications and Information Processing Technology (CAIPT)*, pp. 1-4, 2017.

[17] H. Alquhayz, H. Z. Tufail, B. Raza, "The multi-level classification network (MCN) with modified residual U-Net for ischemic stroke lesions segmentation from ATLAS," *Computers in Biology and Medicine*, vol. 15, p. 106332, 2022.

[18] J. Lee, M. Lee, J. Lee, R. E. Y. Kim, S. H. Lim, D. Kim, "Fine-grained brain tissue segmentation for brain modeling of stroke patient," *Computers in Biology and Medicine*, vol. 15, p. 106472, 2023.

[19] X. Liu, H. Yang, K. Qi, P. Dong, Q. Liu, X. Liu, et al., "MSDF-Net: Multi-scale deep fusion network for stroke lesion segmentation," *IEEE Access*, vol. 7, pp. 178486-178495, 2019.

[20] X. Y. Lee, M. J. Mohamed Mokhtarudin, R. Junid, "Brain lesion image segmentation using modified U-net architecture," in *Intelligent Manufacturing and Mechatronics*, pp. 549-555, 2024.

[21] Y. Zhou, W. Huang, P. Dong, Y. Xia, S. Wang, "D-UNet: A dimension-fusion U shape network for chronic stroke lesion segmentation," *IEEE/ACM Transactions on Computational Biology and Bioinformatics*, vol. 18, no. 3, pp. 940-950, 2021.

[22] Z. Wu, X. Zhang, F. Li, S. Wang, L. Huang, J. Li, "W-Net: A boundary-enhanced segmentation network for stroke lesions," *Expert Systems with Applications*, vol. 230, p. 120637, 2023.

[23] P. Vilela, H. A. Rowley, "Brain ischemia: CT and MRI techniques in acute ischemic stroke," *European Journal of Radiology*, vol. 96, pp. 162-172, 2017.

[24] M. Yanzhen, C. Song, L. Wanping, Y. Zufang, A. Wang, "Exploring approaches to tackle cross-domain challenges in brain medical image segmentation: a systematic review," *Frontier in Neuroscience*, vol. 18, pp. 1-18, 2024.

[25] S. J. Warach, M. Luby, G. W. Albers, R. Bammer, A. Bivard, B. C. V. Campbell, et al., "Acute stroke imaging research roadmap III imaging selection and outcomes in acute stroke reperfusion clinical trials," *Stroke*, vol. 47, no. 5, pp. 1389-1398, 2016.

[26] A. N. Nadzri, N. A. Nik Mohamed, S. J. Payne, M. J. Mohamed Mokhtarudin, "Poroelastic modelling of brain tissue swelling and decompressive craniectomy treatment in ischaemic stroke," *Computer Methods in Biomechanics and Biomedical Engineering*, pp. 1-11, 2024.

[27] A. N. Nadzri, M. J. Mohamed Mokhtarudin, W. N. Wan Ab Naim, S. Payne, "Simulation of craniectomy size in decompressive craniectomy for ischaemic stroke," in *Enabling Industry 4.0 Through Advances in Manufacturing and Materials*, pp. 599-607, 2022.

[28] A. N. Nadzri, M. J. Mohamed Mokhtarudin, W. N. Wan Ab Naim, S. J. Payne, "Simulation of decompressive craniectomy for ischaemic stroke treatment: a conceptual modeling study," in *2020 IEEE-EMBS Conference on Biomedical Engineering and Sciences (IECBES)*, pp. 303-308, 2021.

[29] X. Chen, T. I. Józsa, D. Cardim, C. Robba, M. Czosnyka, S. J. Payne, "Modelling midline shift and ventricle collapse in cerebral oedema following acute ischaemic stroke," *PLoS Computational Biology*, vol. 20, no. 5, p. e1012145, 2024.

[30] F. Yepes-Calderon, J. G. McComb, "Eliminating the need for manual segmentation to determine size and volume from MRI. A proof of concept on segmenting the lateral ventricles," *PLoS One*, vol. 18, no. 5, p. e0285414, 2023.